# Superconducting thin films for Quantum Computing

Evatec's Product Marketing Manager, **Dino Faralli**, and Senior Process Engineers, **Dr. Fiodar Kurdzesau** and **Dr. Yaoxuan Feng**, introduce the quantum qubit application areas requiring thin film deposition and how PVD processes such as evaporation or sputtering can contribute to the future of quantum computing.

### The role of superconductors

Superconducting thin films are key components in the race to build practical quantum computers based on "quantum bits" (or qubit). Different types of qubit devices are under development. Superconducting, photonic, spin-based, and hybrid as well as superconductors like niobium (Nb), NbTi alloys, tantalum (α-Ta), niobium nitride (NbN), and indium (In) provide the backbone for today's leading approaches. Their ability to carry current without resistance makes them ideal for stable qubits, ultra-low-loss resonators, and reliable chip interconnects. To move beyond laboratory prototypes and toward reproducible wafer-scale production, robust solutions for depositing these materials are essential. Physical Vapor Deposition (PVD) processes such as sputtering, evaporation, and co-sputtering/co-evaporation offer exactly this capability. In the following, we share results achieved on Evatec systems that demonstrate how these technologies can accelerate the path from R&D to scalable quantum hardware.

>>>

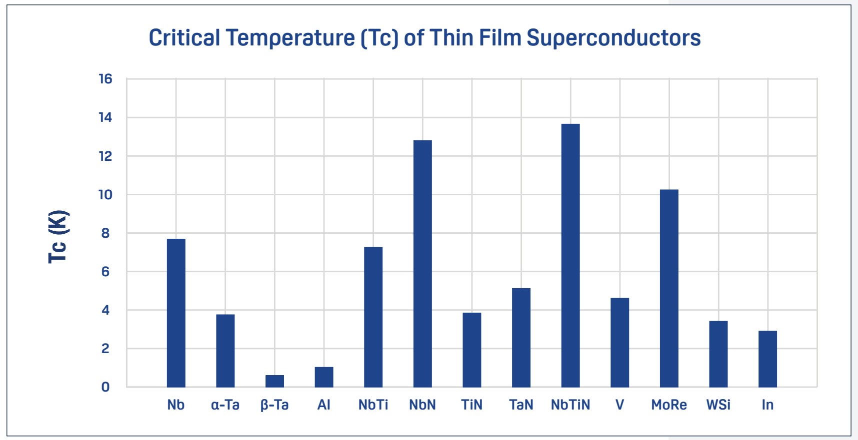


*Figure 1: Critical temperature (Tc) of representative thin-film superconductors. Typical Tc values for elemental films (Nb, α-Ta, β-Ta, Al, In, V), alloys/silicides (NbTi, MoRe, WSi), and nitrides (NbN, TiN, TaN, NbTiN) from sputtered, evaporated, or epitaxial thin films, as reported in literature (Liarte, 2020).*

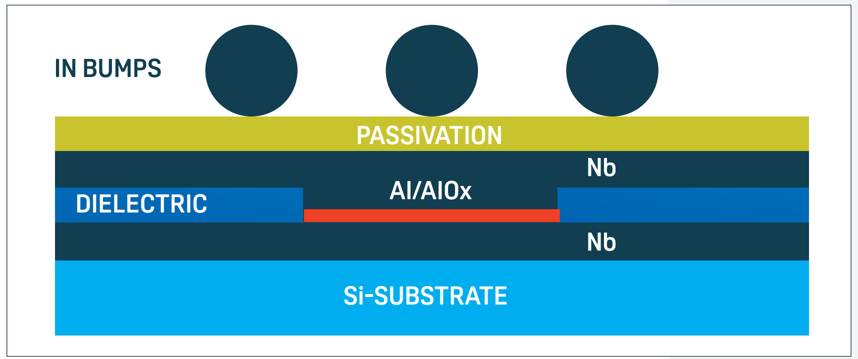


*Figure 2: Schematic cross section of a possible implementation for Josephson-Junction qubits.*

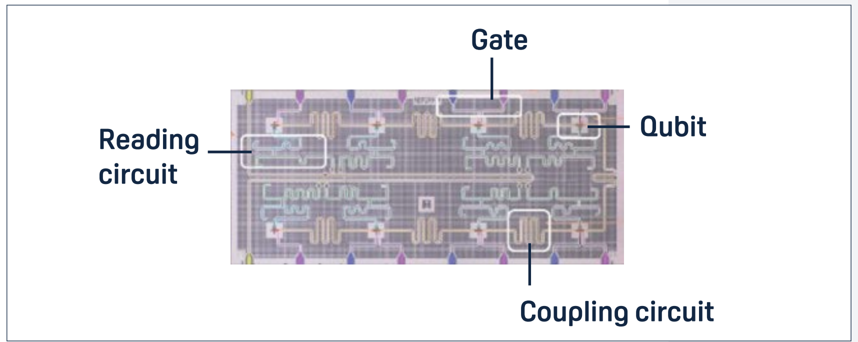


*Figure 3: Superconducting qubit processor from https://qudev.phys.ethz.ch/gallery*

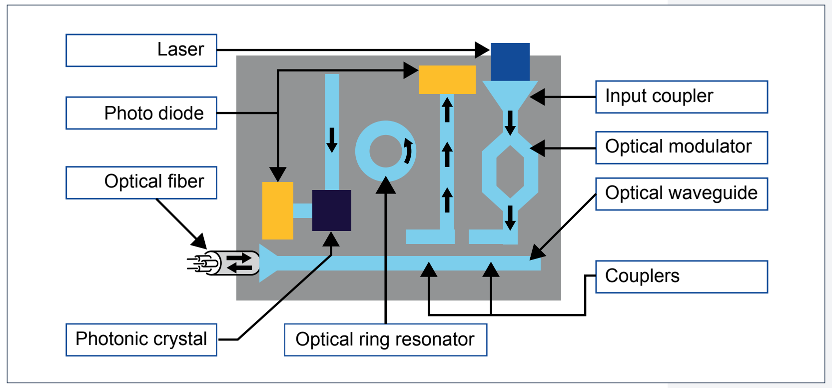


*Figure 4: Schematic view of a possible Photonic Integrated Circuit (PIC)*

## 1. Thin films for Quantum Computing

Superconducting materials deposited by PVD can be integrated into all kinds of quantum qubit technologies. Applications can be grouped into three categories: qubit fabrication, circuit interconnects, and hybrid photonic integration.

- **Qubits:** Niobium and Aluminum are widely used in Josephson junction technology, forming the base electrodes and tunnel barriers. Titanium, Titanium Nitride or NbTi alloys with tailored Ti composition provide tunable Tc values suitable for multilayer qubit stacks.
- **Interconnects**: Indium thin films, with their ductility and low-loss properties, are employed as bump bonds and interconnect layers in multi-chip quantum processors. α-Ta can be used as underlayer for superconducting packaging.
- **Hybrid photonic integration:** Scalable circuits where single-photon sources, waveguides, modulators, detectors, and superconducting elements coexist in a compact architecture. They are gaining attention as "photonic qubits" have been proven at relatively "high temperature" (up to 10K) which may reduce the complexity of the cryogenic system. Evatec has solutions for most of these elements, including: superconductors, as listed above, low-loss dielectrics ($SiO_2$, $Si_3N_4$), LED lasers and photo-diodes (Si, Ge, $HfO_2$, $Al_2O_3$, $NbO_2$, ITO, GZO, GaN), waveguides ($Si_3N_4$, AlN) and piezoelectrics (AlScN, $LiNbO_3$, $BaTiO_3$) for optical couplers and modulators. Among the latter, very good results have been achieved from quasi-epitaxial deposition of $BaTiO_3$ (BTO) using a dedicated off-axis sputtering module at 750°C, with resulting high electro-optic coefficient, comparable to one of MBE grown films. The hardware developed for such modules is shown on page 24, LAYERS 9.

## 2. Sputtering solutions for superconducting thin films

Film properties are shown for Nb and α-Ta sputtered in an Evatec CLUSTERLINE® 200 system on 150mm or 200mm silicon substrates in Figures 6-12. The system was configured as: PVE module for pre-treatment by ICP Ar etch or $H_2$ soft etch; PVD module with ARQ 151 DC source, Nb 300mm target and water-cooled chuck; PVD module with ARQ 151 DC source, 300mm Ta target and "Very Hot Chuck" for heating up to 750°C; degassing unit at temperature up to 250°C; fast cooling station. The crystallographic structure shown in Figure 6 was characterized by XRD. It strongly affects superconducting behavior. For Nb and α-Ta, body-centered cubic (bcc) structures are preferred. Secondary phases need to be avoided, as these can suppress Tc and increase resistivity. Phase and film purity is thus essential for good and stable Tc. High purity sputtering targets (e.g. Nb 5N and Ta 4N5) were used. The system was equipped with UHV Cryo pumps and the PVD modules were pumped to base pressure P=2*10$^{-8}$ mbar before depositions.

### Niobium

Films of thickness 200nm were deposited at nominal room temperature on silicon wafers by DC sputtering, after pre-cleaning by Ar ICP soft-etch. Analysis at XRD shows a polycrystalline film in bcc phase, with (100) peak centered around the expected value ~38.5°, uniform along the wafer diameter (Figure 6).

The deposition rate was set to ~ 2 nm/s at 2 kW DC power. The specific film resistivity at room temperature is ρ ~ 19 µΩ*cm, with measured $R_s$ uniformity within-wafer and wafer-to-wafer less than 1 % (49pts, std dev) on 150mm substrates and 5mm edge exclusion (Figure 7). The superconductive critical temperature (Tc) was evaluated by external partners at values around 9K, in line with state-of-the-art values from literature.

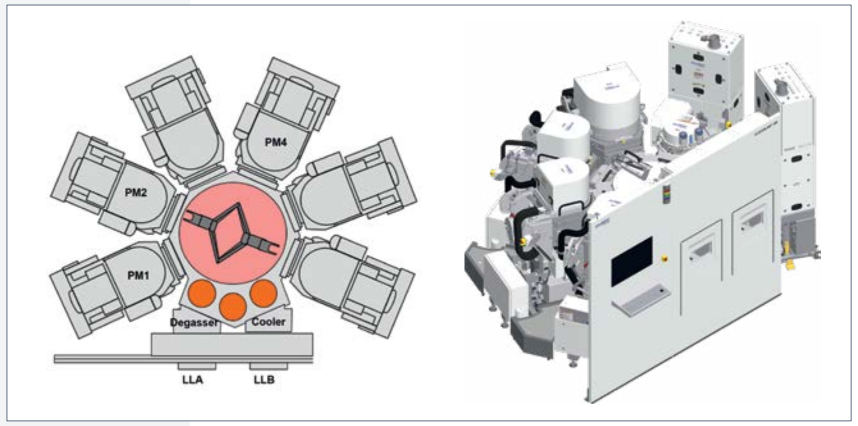


*Figure 5: CLUSTERLINE® 200 system configuration for the deposition of Nb and α-Ta superconductors.*

- **Degasser**
- **PM2, Etch module**
  *Ar ICP etch or $H_2$ etch*
- **PM1, PVD module (Water-cooled chuck)**
  *Target: Nb (5N)*
  *Cathode: ARQ151 DC*
- **PM4, PVD module (VHC)**
  *Target: Ta (4N5)*
  *Cathode: ARQ151 DC*
- **Cooler**

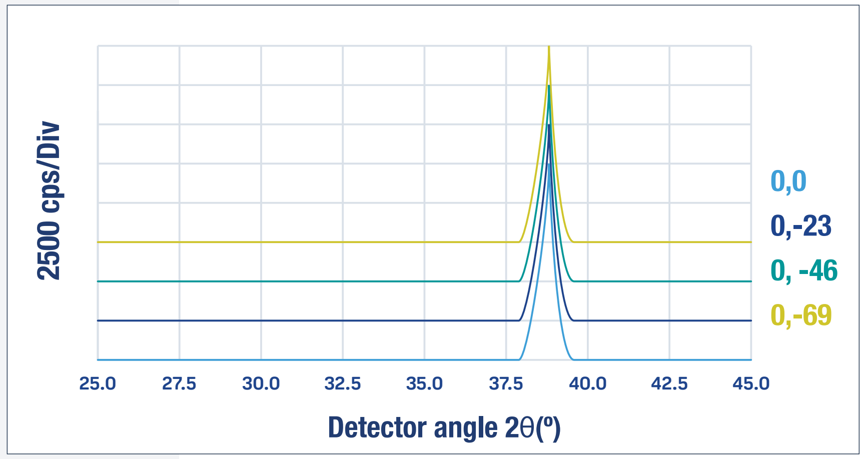


*Figure 6: XRD analysis of Nb 200nm film, in 4 positions along substrate radius, position 0 (center), 23mm, 46mm and 69mm. Peak is centered around 38.5° with good uniformity.*

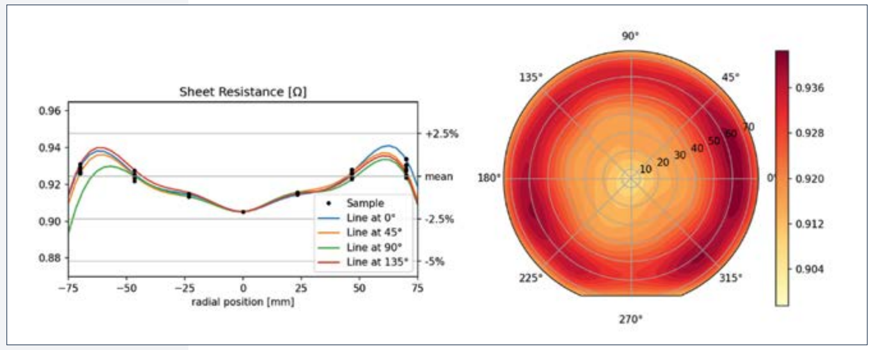


*Figure 7: $R_s$ map and uniformity of Nb 200nm deposited on 150mm silicon substrate.*

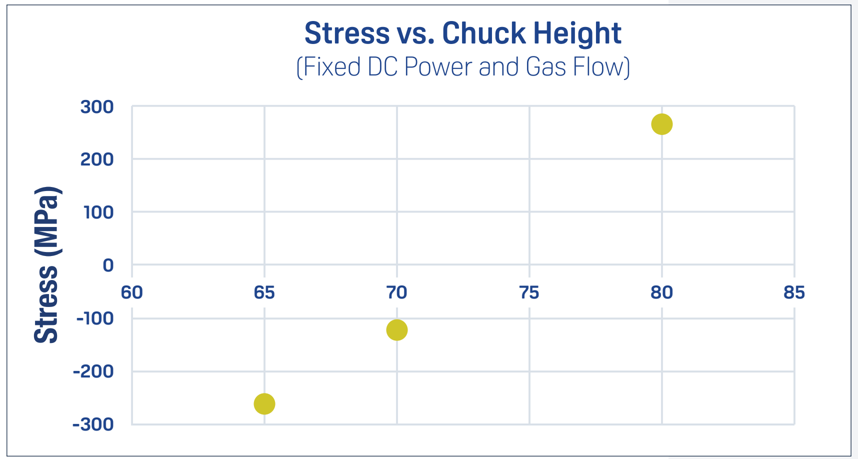


*Figure 8: Nb film stress as a function of the wafer-to-target distance (variable chuck height).*

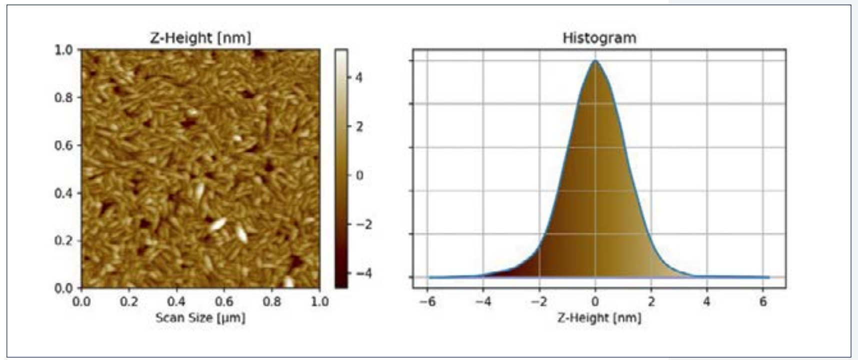


*Figure 9: Nb 200nm film surface roughness measured by AFM in 1x1 mm² area.*

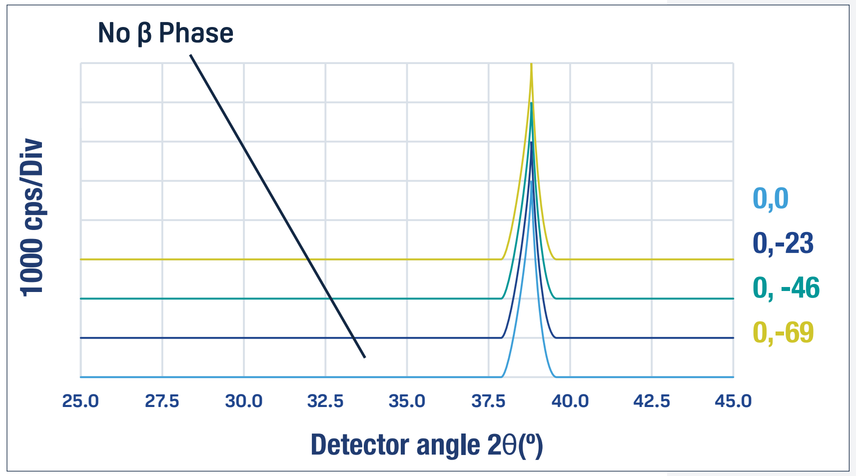


*Figure 10: XRD analysis of Ta 200nm film deposited in pure α-phase @600°C over buffer layer: 4 positions on substrate radius, position 0 (center), 23mm, 46mm and 69mm. Peak is centered around 38.5° with good uniformity.*

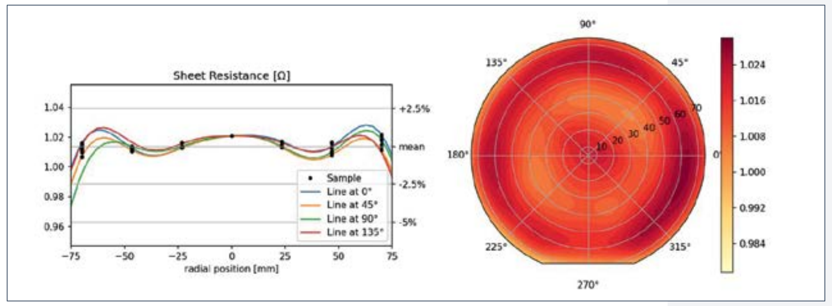


*Figure 11: $R_s$ map and uniformity of α-Ta 200nm deposited @600°C over buffer layer on 150mm silicon substrate.*

Mechanical stress is a key parameter for device integration. Residual film stress at room temperature is usually preferred to be moderately compressive, to keep the stress low at ultra-low operating temperatures, with improvement of the film stability and Tc. Film stress could be tuned over a wide range from tensile to compressive, by tuning the sputtering parameters, like power density, gas flow and chuck height (Figure 8).

Low surface roughness is another key parameter when integrating stack of films at the extremely uniform conditions required by quantum computing e.g. in the formation of barriers for Josephson Junctions. AFM measurements on scan area 1x1 µm area showed a smooth surface with very good Ra ~0.89 nm and Rq ~ 1.1 nm (Figure 9).

## α–Tantalum

For superconducting Tantalum, it is important to deposit it in so-called α-phase, with body-centered cubic (bcc) structure. This is more stable, less resistive and with higher Tc compared to tetragonal β-phase. Deposition at high temperature >500°C is usually enough to get pure α-phase. Films of thickness 200nm were deposited at 550°C and 600°C (using the Evatec "Very Hot Chuck") on silicon wafers by DC sputtering, after pre-cleaning by Ar ICP soft-etch. Analysis by XRD showed a polycrystalline film in bcc α-phase, with (100) peak centered around the expected value 38.5°C, without β-phase peaks. Best results were obtained by deposition on a buffer layer, to avoid interdiffusion of Ta with the silicon substrate at the high deposition temperature (Figure 10). Choosing the appropriate buffer/seed layer leads to pure α-phase even at low deposition temperature.

The deposition rate was set ~ 2.5 nm/s at 2 kW DC power. The specific film resistivity at room temperature was ρ ~ 16 µΩ*cm, with measured $R_s$ uniformity within-wafer and wafer-to-wafer less than 1 % (49pts, std dev) over buffer layer on 150mm substrates and 5mm edge exclusion (Figure 11). The film stress was compressive, with a typical value around -700 MPa (tunable by adjusting sputtering power and gas flow).

The film surface roughness after deposition at 600°C over buffer layer, measured by AFM on scan area 1x1 µm area, showed a smooth surface with very good Ra ~0.81 nm and Rq ~ 1 nm (Figure 12).

## 3. Co-evaporation of superconducting alloys

50 and 100 nm thick NbTi layers with Ti content between 0 and 50 wt.% were deposited within a BAV 1401 evaporation set-up using two different configurations (2xE-Guns and E-Gun+Thermal boat). The wafers were placed on the spherical calotte with 1050 and 700mm radiuses, where two independently driven E-Gun evaporation sources (Figure 13a) or the combination of E-Gun and Thermal Boat (Figure 13c) were installed (one in the geometrical centre of the calotte (in-axis) for Nb and the second, with 220 mm side displacement (off-axis) for Ti), respectively (see Figure 13b). This geometry corresponds to quasi-"lift-off" conditions and allows reaching >80° material incidence angles when keeping the substrates at room temperature conditions. The films were directly grown on Si and $Si/SiO_2$ 4-inch wafers at 0.5-2.0·10⁻⁶ mBar base pressure using neither adhesion nor capping layers.

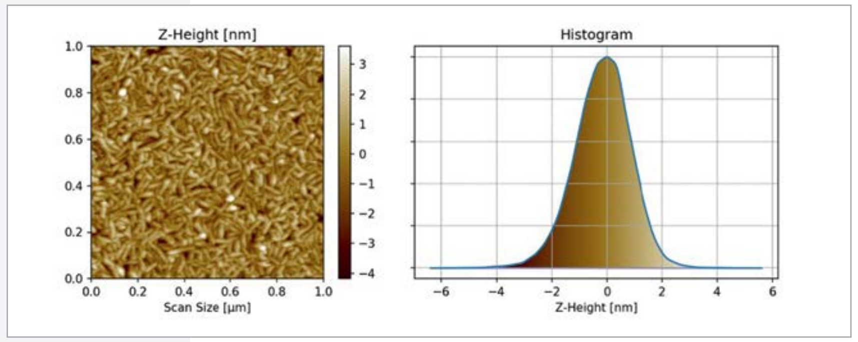


*Figure 12: α-Ta 200nm film surface roughness measured by AFM in 1x1 µm² area.*

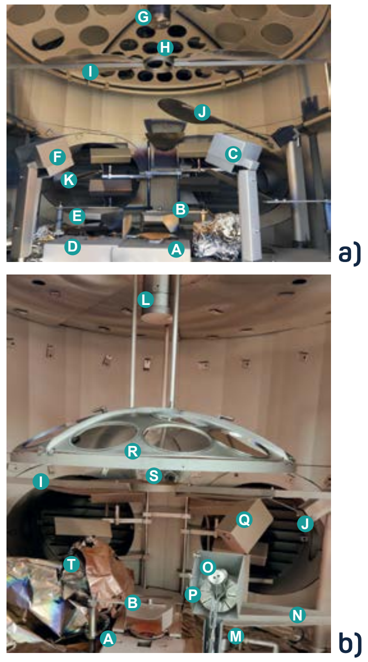


A ESQ 213 central E-gun source (Nb)
B Shutter for central ESQ source
C QSK 300 unit for central ESQ (Nb)
D ESQ 213 side E-gun source (Ti)
E Shutter for side ESQ source
F QSK 300 quartz unit for side ESQ (Ti)
G QSK 1222 quartz unit (monitor)
H Position of sampling wafer(s)
I Fixed 2-fold shaper
J Movable Pivot shaper
K Fixed side shaper (Ti)
L QSK 1221 quartz unit (Nb)
M Thermal boat (Ti)
N Shutter for thermal boat
O QSK 300 quartz unit (Ti)
P Chopper for QSK 300
Q QSK 631 quartz unit (monitor)
R 4x segments calotte R=0.7m
S Thermocouple
T KDC 100 source (covered)

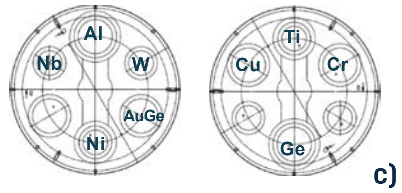


1st E-Gun:
(in-axis for both configurations)

2nd E-Gun:
(configuration 1)

Thermal boat (protected tungsten) filled with Ti (configuration 1)

*Figure 13: BAK system for depositing NbTi superconductor: double E-Guns configuration with 1050 mm sample to source distance (a); material arrangement for the co-evaporation tests (b) and E-Gun+Thermal boat configuration with 700 mm sample to source distance (c).*

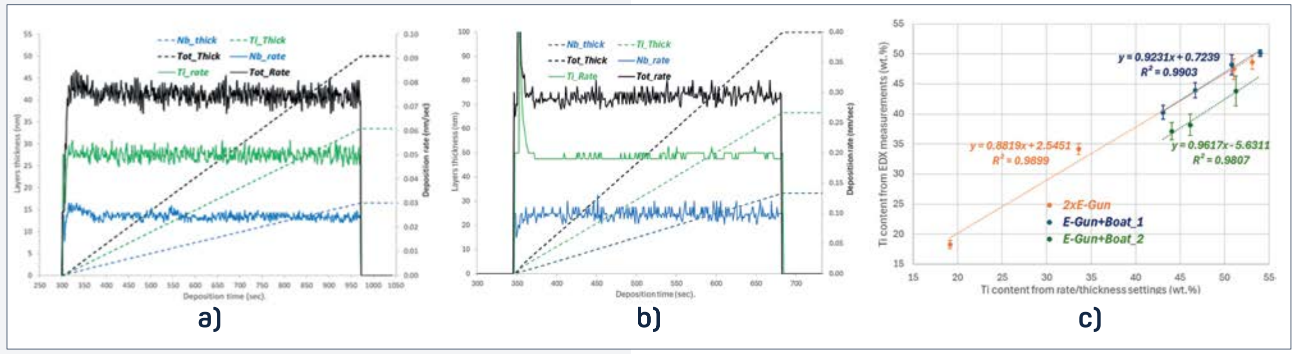


*Figure 14: Adjusting of rate and thickness of co-evaporated layers with monitoring quartz crystals in double E-Guns (a) and E-Gun+Thermal Boat (b) configurations, which allows to create the corresponding process calibration curves (c).*

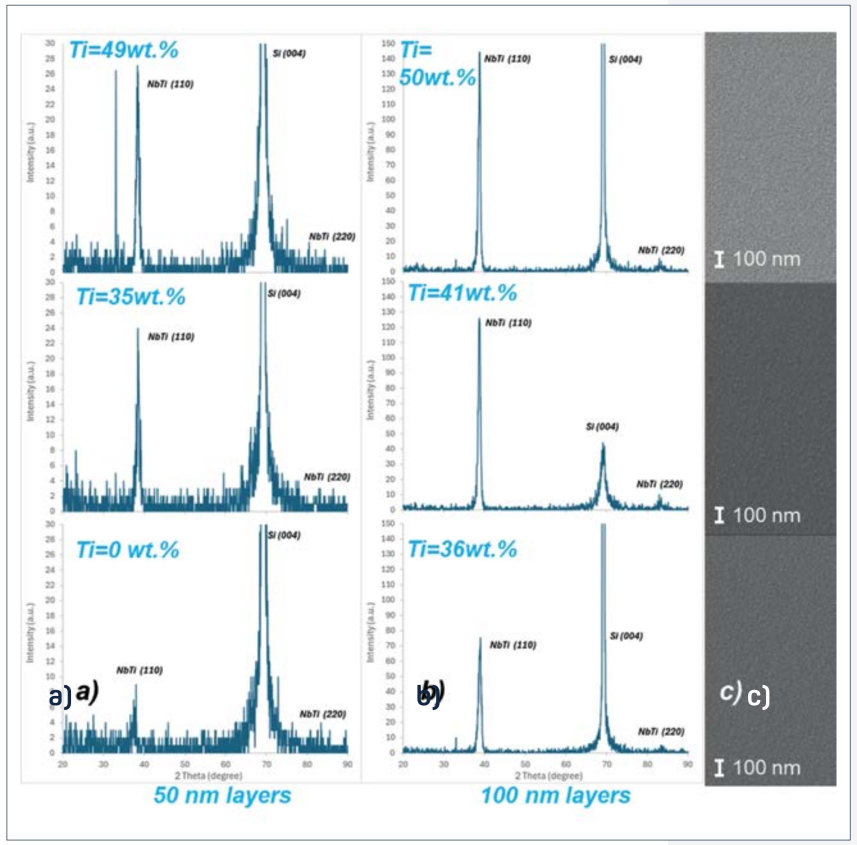


Figure 15: XRD (a, b) and SEM (c) data for NbTi layers from 2xE-gun (a) and E-Gun+Boat (b) processes with 50 and 100 nm thicknesses.

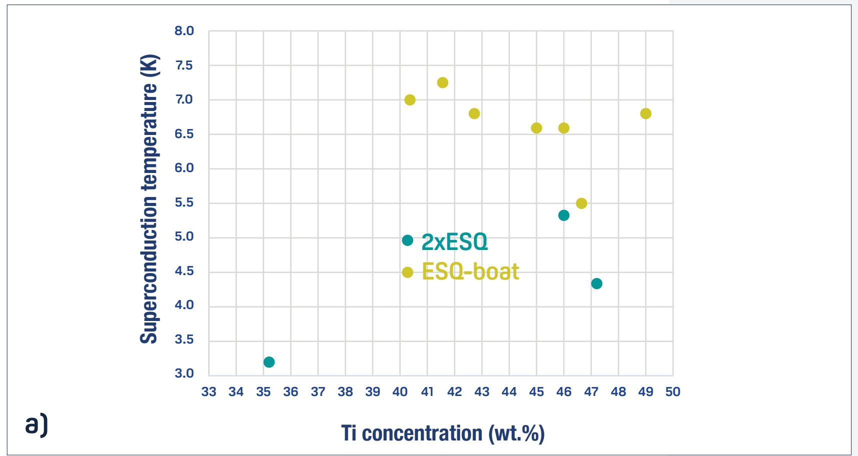


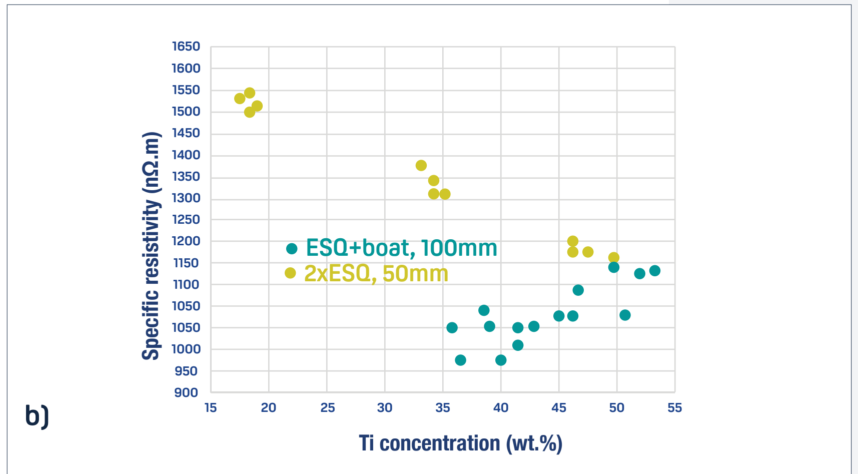


Figure 16: Electrical resistance data: superconducting temperature (a) and specific resistivity (b) as a function of Ti content in co-evaporated NbTi films.

Both co-evaporation techniques used enabled excellent control over the chemical composition of deposited layers. Ti content could be varied in a wide range with good precision by adjusting the deposition rates / thicknesses of co-evaporated Nb and Ti materials (see Figures 14a and 14b) for double E-Guns and E-Gun+Thermal Boat configurations, respectively). The final film composition was verified by EDX measurements, enabling creation and efficient use of corresponding calibration curves for both 2xE-Guns and EGun+Boat configurations (Figure 14c). SEM and XRD analyses confirmed that optimized films exhibit dense structures with increased intensity of NbTi (110) crystalline phase, which also depends on their thicknesses (Figure 15).

The NbTi alloys produced displayed superconducting temperature (Tc) tunability: films having 40–45 wt.% Ti achieved the best performance with Tc ≈ 7.5K. Outside this window, Tc decreased due to the structural disorder or secondary phases (Figure 16a), which also correlates with the layers' specific resistivity values (Figure 16b).

As the long-term stability of superconducting films is critical, corresponding aging tests were also performed. NbTi films with 40–45 wt.% Ti stored under ambient conditions, which simulated two years of device operation, maintained their Tc at a high-level demonstrating robustness against oxidation and contamination (see Figure 17).

Through these results we see that double E-Guns and E-Gun+Boat co-evaporation techniques allow large-scale fabrication of stable superconducting NbTi layers with a variable transition temperature (up to 7.5K). Both processes showed good control and could be used for producing nano- and microscale structures remaining stable in long-term operation at atmospheric conditions. Future process optimization is expected to further improve superconducting temperatures toward the 9K level.

The layers' nitrification by ion-assisted deposition (IAD) in $N_2$ plasma for their conversion into NbTiN form should also be considered, which could enhance Tc above the 13K level [9].

## 4. Future Perspectives

The deposition of superconducting thin films, at critical temperature (Tc) up to 15K, is today available by several manufacturing-ready techniques, including PVD sputtering and evaporation.

Similar hardware as used in standard semiconductor processes can be used to fabricate Qubit devices with both Josephson-Junctions or hybrid Photonics approaches, and deposition technology is ready for volume manufacturing.

Research and development into next generation of superconducting alloys (like NbTiN and MoRe) can also take advantage of the Evatec MSQ (Multi-Source-Quattro, Figure 18) co-sputtering module, which enables DC/DC+ and RF/DC depositions from up to four different 100mm sputtering targets at the same time, in Argon or reactive process gas $N_2$ or $O_2$, at temperature up to 500°C. Development of a new rotating chuck for deposition up to 750°C (e.g. for α-Ta) is ongoing with the expected first prototype in 2026.

Future device productuion needs may benefit from integration of PVD with ALD and CVD thin film capability in the same deposition system. Extension of the deposition technology to 300mm substrates is also on the road map.

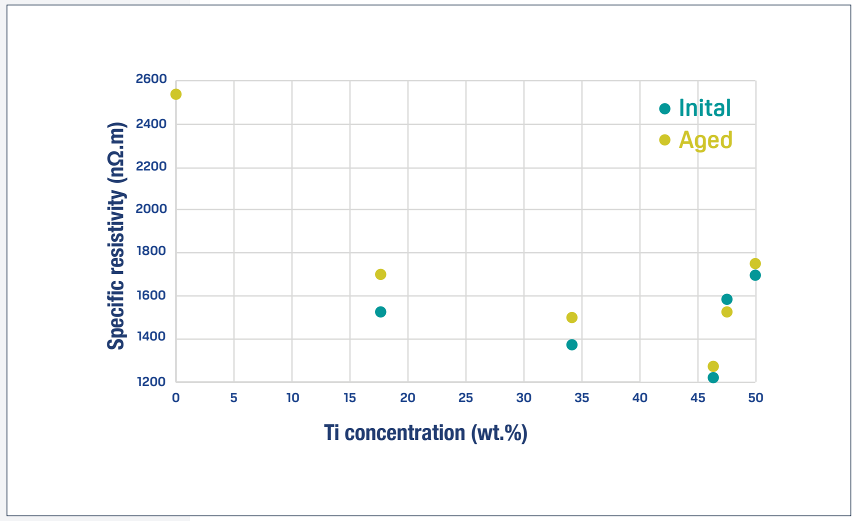


Figure 17: Aging study showing stable specific resistivity of NbTi films after "two years operation" accelerated tests, which correlates with high Tc values (see Figure 16a).

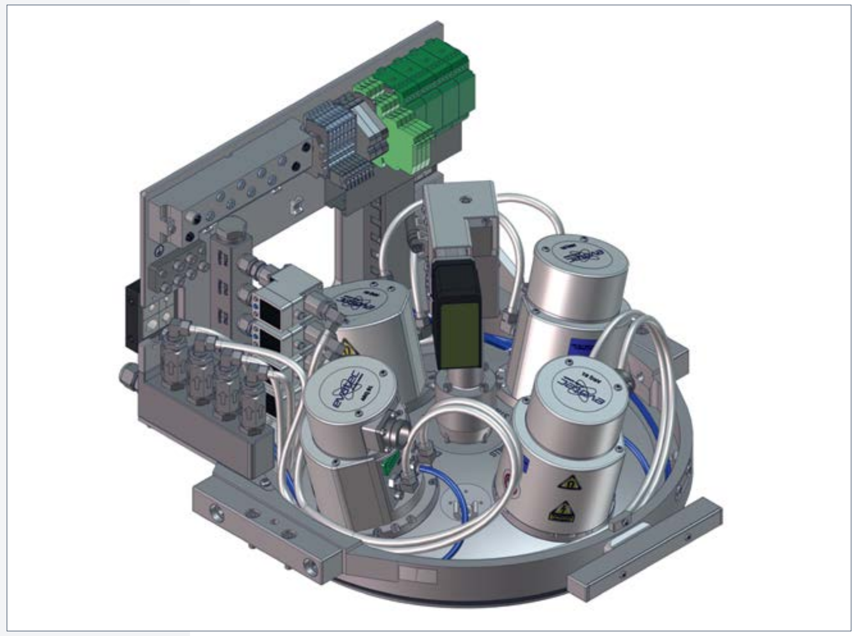

Figure 18: Drawing of the MSQ Multi-Source-Quattro with 3x sources DC/DC+ and 1x source RF/DC for co-sputtering and reactive sputtering of superconductive alloys.

**References:**
[1] Liarte, Supercond. Sci. Technol. 33, 2020. [2] Heinsoo, Phys. Rev. Applied 10, 2018. [3] Kurdzesau, Gabureac, Kratzer, Heinz, 'NbTi Co-evaporation', Poster E-MRS Spring Meeting, 2025. [4] Barends, 'Coherent Josephson qubit,' Nature, 2013. [5] Krantz, 'A quantum engineer's guide to superconducting qubits,' Applied Physics Reviews, 2019. [6] Devoret, Schoelkopf, 'Superconducting circuits for quantum information: an outlook,' Science, 2013. [7] Kjaergaard, 'Superconducting Qubits: Current State of Play,' Annual Review of Condensed Matter Physics, 2020. [8] Oliver, 'Materials challenges in superconducting qubits,' Journal of Materials Research, 2021. [9] Rezinovsky , Hofer, Sirena, Haberkorn, 'Flexible NbTiN thin films for superconducting electronics,' Physica C: Superconductivity and its Applications, Vol. 607, 2023, 1354241.